LAWRENCE
LIVERMORE
NATIONAL
LABORATORY

LLNL-JRNL-659895

Relaxation dynamics of nanosecond laser superheated material inside the surface of dielectrics

S. G. Demos, R. A. Negres, R. N. Raman, M. D. Feit, A. M. Rubenchik

September 5, 2014

OPTICA

Disclaimer

Relaxation dynamics of nanosecond laser superheated material inside the surface of dielectrics

S. G. Demos, R. A. Negres, R. N. Raman, M. D. Feit, A. M. Rubenchik

Lawrence Livermore National Laboratory, 7000 East Ave., Livermore, CA 94551

Abstract

We investigate the dynamics and mechanisms of relaxation of superheated dielectric materials following absorption of nanosecond laser pulses. The experimental results capture the kinetic properties and ejection time of particles generated during the relaxation process, which in turn provide information about the dynamics of the pressure of the superheated material. The results suggest that, microscale particles are generated when the pressure of the material becomes about 4 GPa, the duration of the explosive relaxation process is on the order of 1 μsec. and the relaxation process involves distinct phases.

Intense laser pulses are commonly used in various technology and science applications to deposit energy in a thin near-surface layer of materials generating energy densities well above the evaporation enthalpy. The response of materials as a result of such interaction with ultra short pulses is relatively well understood [1-4] compared to the case of energy deposition with nanosecond pulses. In the later case, a thermal equilibrium is established between the near solid density plasma formed and the lattice while the material becomes thermodynamically unstable. The material responds via an explosive process that has been extensively studied in the context of laser ablation for material processing, chemical analysis, manufacturing of nano-materials or film deposition and laser induced damage in optical components for high power laser systems [5-9].

Measurements of dynamic parameters of these explosive processes such as the expansion of the shockwave and the ionized gas, and kinetics and distribution of ejected and re-deposited particles as a function of laser parameters and energy deposited have been used for gaining insight into the dynamics of the generated ejection plume [10-13]. Experimental evidence and modeling suggest that the material is exposed to pressures on the order of 10 GPa and temperatures on the order of 1 eV [14-16]. Much less information exists on the relaxation of this metastable state, and in particular, the dynamics and mechanisms involved in the relaxation of the overheated material. The relaxation process includes vaporization, particle ejection, radiative cooling and phase transformation. This is a complex problem that is very challenging to be described using current modeling tools.

The work focuses on characterizing (with the necessary temporal resolution) the dynamics of microscopic particles ejected following exposure to ns laser pulses inside the output surface of several dielectrics with widely differing physical properties. We argue that the kinetic properties of the ejected particles provide information about the state of the laser superheated material at the time of separation of the particles, which in turn can be used to probe the relaxation dynamics of the laser superheated material. This approach provides, for the first timer to our knowledge, experimental evaluation of the temporal relaxation of the overheated matter.

A schematic diagram of the time resolved shadowgraphic imaging system utilized in this work is shown in Figure 1. This system has been described in detail elsewhere [17,18]. In brief, breakdown was induced on the exit (output) surface of the samples using a “pump” laser pulse obtained from two laser systems. The first “pump” laser source was operating at 355 nm with pulse duration of 3-ns full-width at half maximum (FWHM). The second “pump” laser source was operating at 1064 nm with pulse duration of 10-ns full-width at half maximum (FWHM). The breakdown was induced by focusing a laser pulse behind the exit-surface of transparent samples at fluences on the order of 40-60 J/cm^2 and 200-300 J/cm^2 for the 355 nm and 1064 nm pump lasers, respectively. The surface of the sample was exposed to a nearly Gaussian beam profile having 1/e^2 beam diameter on the order of 50-150 μm, differently adjusted in each material aiming at producing similar

ejected particle jets, typically on the order of 50-80 μm in diameter. All experiments were performed in ambient air.

Two spatially overlapped, orthogonally polarized 532 nm, 4.5 ns FWHM *probe* laser pulses were used to illuminate the location of energy deposition parallel to the surface of the sample as shown in Figure 1. Each probe pulse was delayed independently with respect to the peak of the pump pulse via adjustable external triggers, allowing side-view illumination of the sample at two time points following a single laser energy deposition event. A composite 5X zoom and objective (5X or 2X) lens system was used to collect the dual-probe signal traversing the ejected material volume; this signal was subsequently passed through a 532-nm narrowband filter and separated into its constituent polarization components using a polarizing beam-splitter. This made possible to capture images of the ejected material at two different delays for a single event using separate charge-coupled device (CCD) cameras. Static optical resolution was better 1-2 μm with a depth of focus of ~20-40 μm, depending on the choice of the objective.

We have evaluated an array of transparent dielectric materials representing a wide range of band gap energies and mass densities (~2.7-12 eV and ~2-8.4 g/cm^3, respectively). The samples were optical flats, typically with a thickness on the order of 1 cm. In some of these materials (or perhaps the specific samples we utilized) we were not able to initiate breakdown inside the exit surface and the ensuing formation of a jet of ejected particles because the plasma was forming either inside the bulk or sometimes substantially below the surface. In the later case, the eruption through the surface yielding larger particles of very low speeds was significantly delayed and were considered outside the focus of this study. Consequently, the materials included in this study were the following: fused silica (SiO_2), sapphire (Al_2O_3), zinc selenide (ZnSe) and lead tungstate crystals ($PbWO_4$). We also included calcium fluoride (CaF_2) and DKDP ($KH_{2-x}D_xPO_4$) crystals in which the early material ejection process was dominated by the generation of gaseous material well visualized by our experimental apparatus.

The motivation for generating breakdown on the exit surface of the samples is two-fold. First, we wanted to avoid the interaction of the laser pulse with the expanding

plume which causes instabilities on the absorption front in order to enable direct observation of the spontaneous reaction of the host material [13,19]. Second, upon initiation of breakdown on the exit surface, the absorption front moves into the bulk material generating a substantial volume of partially confined superheated material. This offers an ideal experimental model for capturing the superheated material response and relaxation.

Typical experimental results are shown in Figures 2a and 2b capturing the individual ejected particles and the shockwave propagating in the air for each material at 950 nsec delay (from the peak of the pump pulse) for the case of Al_2O_3 and $PbWO_4$, respectively. The location of the leading edge of the jet in each material was determined by obtaining an average value of the location of the visible particles most distant from the surface over a large number of measurements. In this set of measurements, the 2X objective was used in order to maximize the image field of view to better capture the shockwave and particle jet leading to visualization of particles having diameter of about 1.5 μm or larger. Images of the ensuing damage sites revealed a similar size and general structure of the resulting (from the material ejection process) crater in all samples.

Figure 2c shows the distance traveled by the leading edge of the jet in each material and the corresponding kinetic energy density as a function of the material density (2.20, 3.98, 5.57 and 8.34 g/cm^3 for SiO_2, Al_2O_3, ZnSe and $PbWO_4$, respectively). The results indicate that although the speed of the ejected particles is affected by the density of the host material, the estimated kinetic energy density of the particles forming the leading edge of the particle jet is for all materials within a very narrow range at about 3 GJ/m^3. This energy is few times smaller then the evaporation energy, which is on the order of 10 GJ/m^3 or higher [20], but well above the melting enthalpy giving rise volume boiling It has been proposed that the particle ejection process is due to the fact that the energy density deposited in the material is so high that the material becomes locally thermodynamically unstable, producing a bubble-liquid mixture [5-9]. Therefore, particles may be ejected over the entire period of time of relaxation of the superheated material until the thermodynamic stability is reached. It is logical to assume that the internal energy of the particle remains unchanged during its separation from the

superheated material. Consequently, the kinetic energy of the particle arises from pV work of the ejected material volume. As a result, the estimation of the kinetic energy density of the ejected particles can provide a first order approximation of the pressure of the superheated material at the time of ejection of the particle. This implies that the kinetic properties of the ejected particles provide an indication of the state of the laser superheated material. The results shown in Figure 2c suggest that the kinetic energy density of the particles forming the leading edge of the jet in all material tested is approximately the same. This in turn suggests that the pressure of the superheated volume in this set of materials is on the order of 3.1 GPa at the time of ejection of the most energetic particles observed with this experimental system.

The capability of our experimental system to acquire two images at different delays from the same event can be used to more accurately calculate the speed of the ejected particles [17,18] but more importantly, to estimate the time of ejection of each particle from the surface. Consequently, the ability of the system to enable an estimation of the ejection time can be used to probe the relaxation process of the plasma superheated material. To test the concept, we measured the particle speed as a function of the estimated ejection time for the case of exit surface breakdown in fused silica using the experimental parameters adapted in previous reports [18, 21] under 355 nm, 3 ns irradiation (as discussed earlier and shown in Fig. 1) and fluences on the order of 40-60 J/cm^2. These excitation conditions create breakdown from preexisting defects, commonly referred to as laser damage, confined to very small areas generating a particle ejection jet where individual particles can be tracked using our experiment system. The 5X objective was used to acquire this set of images which allowed us to detect smaller particles having diameter of about 1 μm and higher speeds of about 2 Km/sec (compared to the 2X objective used to obtain the results shown in Fig 2). The results are shown in Figure 4 indicating that the material ejection process is longer than 1 μsec as it has been previously suggested using a different approach [18]. These results were compiled using images that captured different breakdown events under nominally identical excitation conditions. Nearly spherical particles that were clearly visible in the images at both delays (in focus with no obscuration or interference form other particles) that were

located at a distance between 60 and 250 μm from the surface during image acquisition were selected while larger high aspect ratio (such as flakes) particles were not included.

The observed ejected particle jet represents the non-gaseous component of the ejection plume. On the other hand, the observed shockwave (see Figure 2) represent the boundaries on the ejection plume. The typical size of a particle is a few microns. The particle with radius *a* moving with a speed *v* relative to the gaseous component of the plume which has viscosity η is slowed down by the Stokes drag force $6v\pi\eta a$. During the first few μsec, the gaseous plume also expands. However, for the sake of simplicity, let us assume that the relative velocity *v* is equal to the initial speed of the particle *V* (surrounding gas is not moving). In this case, the instantaneous speed *v(t)* can be expressed as $v(t) = V\exp(-t/\tau)$ where $\tau = 2\rho a^2/9\eta$ and the dynamic viscosity of air is η=0.00018 g/sec cm. This yields that even for the smallest particles observed in our system, there will be less than 5% change in the speed of the particles within the first microsecond. Therefore, the speed of the particles as estimated by our experimental system (see Figure 3) is nearly the same as at the moment of ejection from the superheated material.

The corresponding kinetic energy density of the particles is also presented in Figure 3. The results indicate that the kinetic energy of the particles monotonically decreases with the ejection time of the particles. This effect is also captured empirically in the time resolved images as all particles located at the same distance from the surface have identical velocities and particles never overtake one another [21]. As mentioned earlier, a detailed modeling of this process is not possible mainly because the underlying processes involved remain unclear. In order to elucidate these processes, we attempted an empirical fit of the data using a double exponential decay function:

$$K = c_0 + c_1 \times \exp\left(\frac{-(t-t_0)}{\tau_1}\right) + c_2 \times \exp\left(\frac{-(t-t_0)}{\tau_2}\right) \qquad (1)$$

where *K* is the kinetic energy density (in J/m^3) of the particles, *t* is the time (in ns), t_0 is the delay time for the onset of particle ejection, τ_1 and τ_2 are decay time constants while

c_1, c_2 and c_3 are fitting constants. The fit to the data shown in Figure 3 was obtained using the following fitting parameters:

$$c_0 = 4\times10^5\ J/m^3,\ c_1 = 3.8\times10^9\ J/m^3,\ c_2 = 9\times10^7\ J/m^3,$$
$$t_0 = 30\ ns,\ \tau_1 = 15\ ns,\ \tau_2 = 170\ ns \qquad (2)$$

Previous work suggested that the material ejection process was prolonged [18]. Recent work also demonstrated that during breakdown on the exit surface of fused silica using 355 nm laser pulses, there is an initial swelling of the surface with the ejection of particles starting at about 35 ns delay [21]. The fit to the experimental data shown in Figure 4 suggests that there is a delay t_0 = 30 ns before the ejections of particles, which is in agreement with this previous report. Furthermore, two decays times (τ_1 and τ_2) are suggested indicating two different mechanisms of material ejection with lifetimes of about 15 and 170 ns respectively. This behavior will be discussed later in more detail.

Additional information was obtained from the two materials where the gaseous component of the ejection plume was also visualized, namely, in CaF_2 and DKDP. Time resolved images capturing the material ejection process at 150 ns delay under 1064 nm, 10 ns at FWHM, ≈250 J/cm^2 average fluence in CaF_2, and DKDP are shown in Figures 4a and 4b respectively. The shockwave is visible in both cases indicated with arrow #1. The shockwave is also visible in the corresponding image from SiO_2 shown in Figure 4c having traveled a fairly similar distance, an indication that the initial energy deposited was approximately the same during the laser-induced breakdown events. The gaseous material is clearly visible in the case of CaF_2 as a darker feature (indicated by arrow #2) arising from the presence of nanoparticles, as it has been discussed in detail elsewhere elsewhere [22]. In the case of DKDP, the gaseous material is visible from the variation in the intensity of the transmitted light behind the shockwave arising from changes of refractive index at the boundaries of the gaseous material. The outlines of these variations are similar to the boundaries of the observed gaseous material in CaF_2.

The ejected material in the form of particles with diameter on the order of 1-10 μm is observed in DKDP and SiO_2 and is denoted by arrow #3. These images also reveal a secondary event occurring after the initial formation of the shockwave. Specifically, the time resolved image in CaF_2 shows that the gaseous jet of ejected material behind the originally ejected material (having the classical appearance of a "mushroom cloud") is interrupted by a secondary front of gas ejection as indicated by arrow #4. A similar observation is present in DKDP where the secondary ejection seems to generate a second shock-front as indicated by arrow #4 in Figure 4b. Neither of these features are observable in SiO_2 due to lack of imaging contrast, but the particle jet is positioned behind the distance from the surface of the secondary front (as observed in CaF_2 and DKDP). We therefore hypothesize that the particle ejection in SiO_2 follows this secondary explosion.

These observations may be interpreted as the fingerprint of a sequence of phases of the material response to laser energy deposition. Initially, the laser heated material near the surface causes a directional ejection of gaseous material supporting the formation of a shockwave as it has been discussed in more detail in Ref 22. During this time, the surface is swelling encapsulating the superheated material below the surface. This swelling appears as a bulge on the surface followed by the explosive fragmentation of the bulge after about 30 ns delay has been observed for the case of SiO_2 as reported in Ref. 21. This suggests that the confined superheated material is explosively disintegrating with additional directional ejection of gaseous material creating a secondary front (arrow #4 in Figures 4a and 4b). This lowers the superheated material temperature which can then support the formation of a jet of particles in addition to the production of gaseous material. This causes the delay in the ejection of particles reported in Ref 21 and suggested by the fitting parameter of t_0=30 ns for the experimental results of Figure 4.

The fitting parameter τ_1 =15 ns (see eq. 2) may then correspond to the relaxation of the superheated material responsible for the generation by this secondary explosion of the first wave of particles, having higher speed and smaller size. This secondary eruption that

includes the ejection of hot particles causing a cooling of the superheated material and resulting in a decrease with time in the pressure of the bubble-liquid mixture and the energy of the ejected particles. It must be noted that in previous work we reported experimental evidence that the temperature of the ejected particles in SiO_2 under similar excitation conditions are on the order of 0.5 eV [23], well within the temperature range of thermodynamic instability.

Figure 4 indicates that particles are ejected for longer that 1 μsec but they exhibit a low kinetic energy density (captured by the constant c_0 in the fit of eq. 1). This behavior may be associated with the ejection of adjoining pulverized mechanically damaged material that is removed under the stress stored on the material and as the material is cooling within and around the location of energy deposition [21]. Therefore we hypothesize that the particle ejection during the relaxation of the superheated material terminates about 1 μsec after laser energy deposition. During this time. particles are continuously ejected, but with monotonically decreasing speed, capturing the decreasing pressure of the superheated material during this time. This observed cooling time (until reaching the equilibrium liquid state with arrest of particle ejection) is much shorter than assuming only the thermal diffusion time. This means that the cooling process via evaporation and hot particle ejection continues until a thermodynamically stable liquid phase if reached in about 1 μsec delay. Therefore, the fitting parameter τ_2 =170 ns may correspond to the material relaxation until the equilibrium liquid state is reached.

The qualitative model discussed above may suggest that particle ejection is occurring only after the material reaches a pressure (and corresponding temperature) threshold. This threshold may depend on the material. Experiments in DKDP, which has a very low boiling temperature (~ 400 C° in KDP vs. ~2300 C° in SiO_2), show that the initial response of the affected superheated material is quite different and involves the production of gaseous material while, in contrast, SiO_2 (and other material studied) can support production of liquid droplets from early delays. As a result, only the peripheral regions of the heated region in DKDP where the temperature is considerably lower can support formation of micro-scale particles. These particles are ejected in a conical pattern in the presence of the

expanding gaseous material from the central region as has been discussed in more detail in Ref 24. On the other hand, assuming that the particles are produced when the pressure/temperature of the material drops below certain value, the particle jet generated in SiO_2 must have the same kinetic profile independent of the amount of laser energy deposited in the material (initial pressure). To test this concept we performed experiments exemplified in the case example presented in Figure 3 for fused silica showing the images of particle jets at 450 ns delay under exposure to 300 J/cm^2, 10 ns, 1064 nm and 15 J/cm^2, 3 ns, 355 nm laser pulses. The arrows indicate the location of the shockwave in the air revealing a more than two fold difference in the distance traveled between the two cases .

To provide a first order approximation analysis of the result, we can use the theory of point explosion [25]. The position of the shock R is related to the released energy E at moment t by the relation $R=(2.4E/\rho)^{1/}5\ t^{2/5}$. Using the ratio of the laser energies of each pulse (300 J/cm^2 over 15 J/cm^2) the ratio of the distances traveled by the corresponding shock is $20^{1/5}$ =1.82 which is very close to the value observed experimentally. On the other hand, the location of the leading edge of the particle jet remains practically the same (within the size of particles that can be observed with our experimental system) as indicated by the vertical line in Figure 3. This observation seems to support the hypothesis that there is a threshold material pressure for the production of particles.

Summarizing our experimental observations we conclude that there is a prolonged relaxation process until thermodynamic equilibrium of the laser superheated dielectric is reached in a time on the order of 1 μsec in SiO_2. The first phase of the process involves surface explosion that supports the expansion of the shockwave. The second phase involves the explosive eruption of the subsurface confined superheated material accompanied by the ejection of microscopic particles. This second phase was found to occur in the case of SiO_2 with a delay of about 30 ns. The fitting parameter c_1 suggests that the initial ejection of particles occurs when the pressure is reduced to about 3.8 GPa and is similar in other materials studied (see Fig. 2c). The third phase corresponds to the continuation of the ejection of particles until stable liquid phase is established. The fitting parameter c_2 suggests that this phase starts when the energy density is reduced (following

the explosive eruption and material ejection of phase 2) to about 90 MPa. The third phase (clearly observed after the termination of the second phase) involves the ejection of mechanically damaged material that is ejected with speeds on the order of 20 m/sec or less. The fitting parameter c_o suggests that the termination of the second phase occurs when the pressure is reduced to about 0.4 MPa, which is about 4 times the atmospheric pressure.

In conclusion, the results presented in this work suggest that the relaxation process of the laser superheated material includes; a) A surface explosion inducing the shock and gaseous material ejection; b) Delayed secondary eruption of liquid from below the surface confined superheated material; c) Ejection of liquid and mechanically detached material. The delay of the secondary eruption is on the order of a few 10s of ns while the arrest of ejection occurs at a delay on the order of 1 μsec.

Acknowledgments

This work was performed under the auspices of the U.S. Department of Energy by Lawrence Livermore National Laboratory under Contract DE-AC52-07NA27344. [LLLNL-JRNL-659895]

References

1. K. Sokolowski-Tinten, J. Bialkowski, A. Cavalleri, and D. von der Linde, A. Oparin and J. Meyer-ter-Vehn, S. I. Anisimov, "Transient States of Matter during Short Pulse Laser Ablation", Phys. Rev. Lett. 81, 224, 1998
2. B. J. Siwick, J. R. Dwyer, R. E. Jordan, R. J. Dwayne Miller, "An Atomic-Level View of Melting Using Femtosecond Electron Diffraction", Science 302, 1382, 2003
3. D. M. Fritz, et al., "Ultrafast Bond Softening in Bismuth: Mapping a Solid's Interatomic Potential with X-rays" Science 315, 633, 2007
4. N. Zhang, X. Zhu, J. Yang, X. Wang, M. Wang, Mingwei, "Time-resolved shadowgraphs of material ejection in intense femtosecond laser ablation of aluminum", Phys. Rev. Lett. 99, 167602, 2007
5. F. W. Dabby, U-C. Peak, "High-Intensity Laser-Induced Vaporization and Explosion of Solid Material", IEEE J Quant. Electr. 8, 106, 1972
6. Miotello, R. Kelly, "Laser-induced phase explosion: new physical problems when a condensed phase approaches the thermodynamic critical temperature", Appl. Phys. A 69,1999
7. N.M. Bulgakova**1**, A.V. Bulgakov**, "**Pulsed laser ablation of solids: transition from normal vaporization to phase explosion", Appl. Phys. A 73, 199–208 (2001)
8. P. Lorazo, L.J. Lewis, Meunier, Lorazo, P; Lewis, M. Meunier, "Thermodynamic pathways to melting, ablation, and solidification in absorbing solids under pulsed laser irradiation, Phys. Rev. B, 73, 134108, 2006
9. E. Leveugle, A. Sellinger, J. M. Fitz-Gerald, L. V. Zhigilei, "Making Molecular Balloons in Laser-Induced Explosive Boiling of Polymer Solutions", Phys. Rev. Lett. 98, 216101, 2007
10. R. F. Wood, K. R. Chen, J. N. Leboeuf, A. A. Puretzky, and D. B. Geohegan, "Dynamics of Plume Propagation and Splitting during Pulsed-Laser Ablation", Phys. Rev. Lett. 79, 1571-1574, 1999
11. S. S. Harilal, C. V. Bindhu, M. S. Tillack, F. Najmabadi, and A. C. Gaeris, "Internal structure and expansion dynamics of laser ablation plumes into ambient gases", J. Appl. Phys. 93, 2380 (2003)
12. Z. Chen, A. Bogaerts, "Laser ablation of Cu and plume expansion into 1 atm ambient gas", J. Appl. Phys. 97, 063305 (2005)
13. Q. Ma, V. Motto-Ros, Xueshi Bai, J. Yu, "Experimental investigation of the structure and the dynamics of nanosecond laser-induced plasma in 1-atm argon ambient gas", Appl. Phys. Lett. 103, 204101 (2013)
14. A. Salleo, S. T. Taylor, M. C. Martin, W. R. Panero, R. Jeanloz, T. Sands, and F. Y. Genin, Nat. Mater. **2**, 796 (2003).
15. C. H. Li, X. Jua, J. Huang, X. D. Zhou, Z. Zheng, X. D. Jiang, W. D. Wu, and W. G. Zheng, Nucl. Instrum. Meth. B **269**, 544 (2011).
16. M. J. Matthews, C. W. Carr, H. A. Bechtel, and R. N. Raman, Appl. Phys. Lett. **99**, 151109 (2011).
17. Rajesh N. Raman, Raluca A. Negres, Stavros G. Demos, "Time-resolved microscope system to image material response following localized laser energy deposition: exit surface damage in fused silica as a case example," Opt. Eng. **50**, 013602, 2011
18. R. N. Raman, R. A. Negres, and S. G. Demos, "Kinetics of ejected particles during laser-induced breakdown in fused silica", Appl. Phys. Lett. **98**, 051901, 2011
19. X. Bai, Q. Ma, V. Motto-Ros , J. Yu, D. Sabourdy, L. Nguyen, A. Jalocha, J. Appl. Phys., **113**, 013304 (2013).

20. Dieter Bauerle, “Laser Processing and Chemistry”, Spinger-Verlag Berlin Heidelberg 2011
21. Stavros G. Demos, Raluca A. Negres, Rajesh N. Raman, Alexander M. Rubenchik, Michael D. Feit, “Material response during nanosecond laser induced breakdown inside of the exit surface of fused silica”, Laser and Photonics Rev **7**, 444-452, 2013
22. Stavros G. Demos, Raluca A. Negres, Alexander M. Rubenchik, “Dynamics of the plume containing nanometric-sized particles ejected into the atmospheric air following laser-induced breakdown on the exit surface of a CaF_2 optical window”, Appl. Phys. Lett. **104**, 031603 (2014)
23. Rajesh N. Raman, Selim Elhadj, Raluca A. Negres, Manyalibo J. Matthews, Michael D. Feit, and Stavros G. Demos, “Characterization of ejected fused silica particles following surface breakdown with nanosecond pulses”, Opt. Express **20**, 27720 (2012)
24. S. G. Demos, R. A. Negres, R. N. Raman, A. M. Rubenchik, M. D. Feit, “Comparison of material response in fused silica and KDP following exit surface laser- induced breakdown”, Proc. of SPIE **8885**, 88850W-1, 2013
25. Ya. B. Zeldovich, Yu. P. Raizer, “Physics of Shock Waves and High Temperature Hydrodynamic Phenomena”, Academic Press, New York,1967

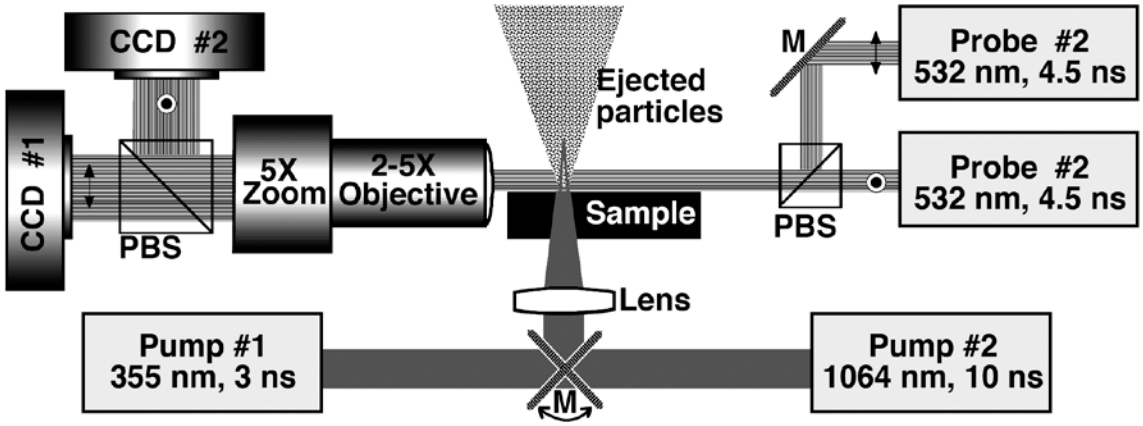

Figure 1: Schematic layout of the experimental system

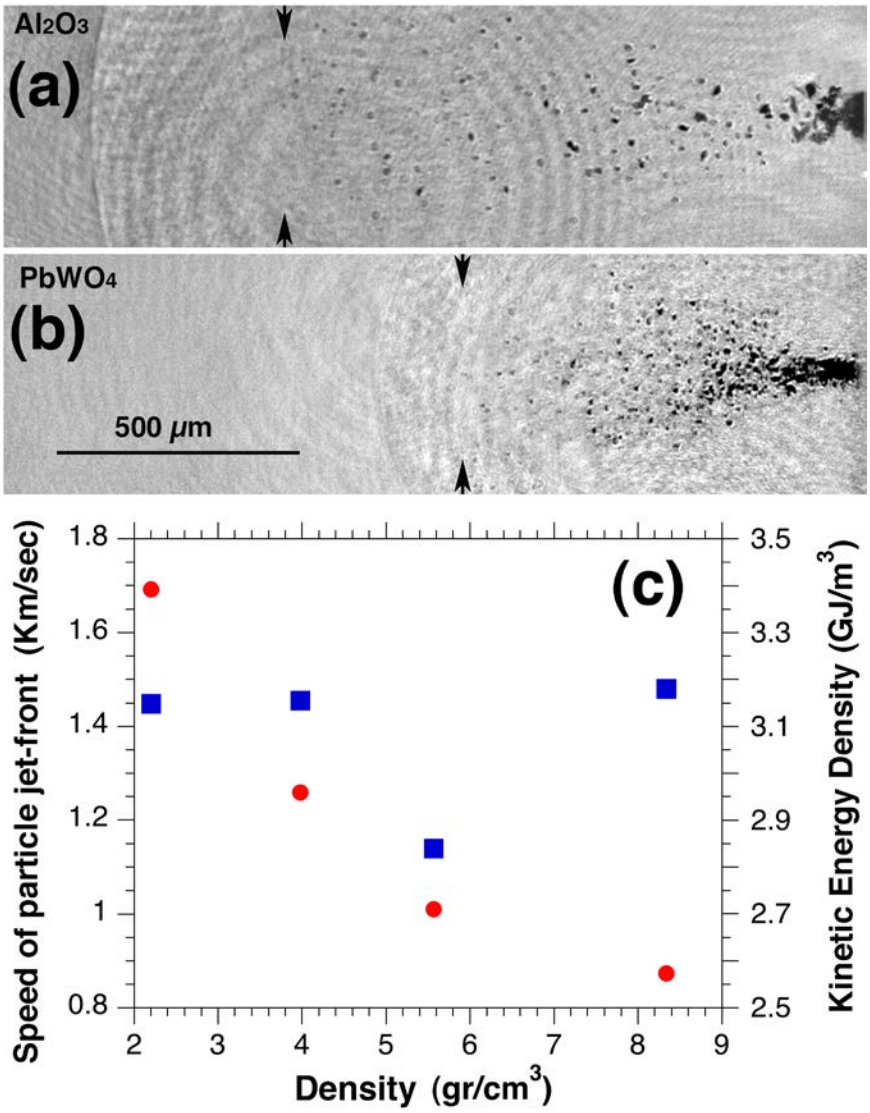

Figure 2: Representative images at 950 ns delay following laser induced breakdown inside the exit surface of a) Al_2O_3 and b) $PbWO_4$. c) The speed of the front edge of the jet of ejected particle (solid circles, shown with arrows in the images) along with the estimated kinetic energy density (open circles) as a function of specific gravity of each material

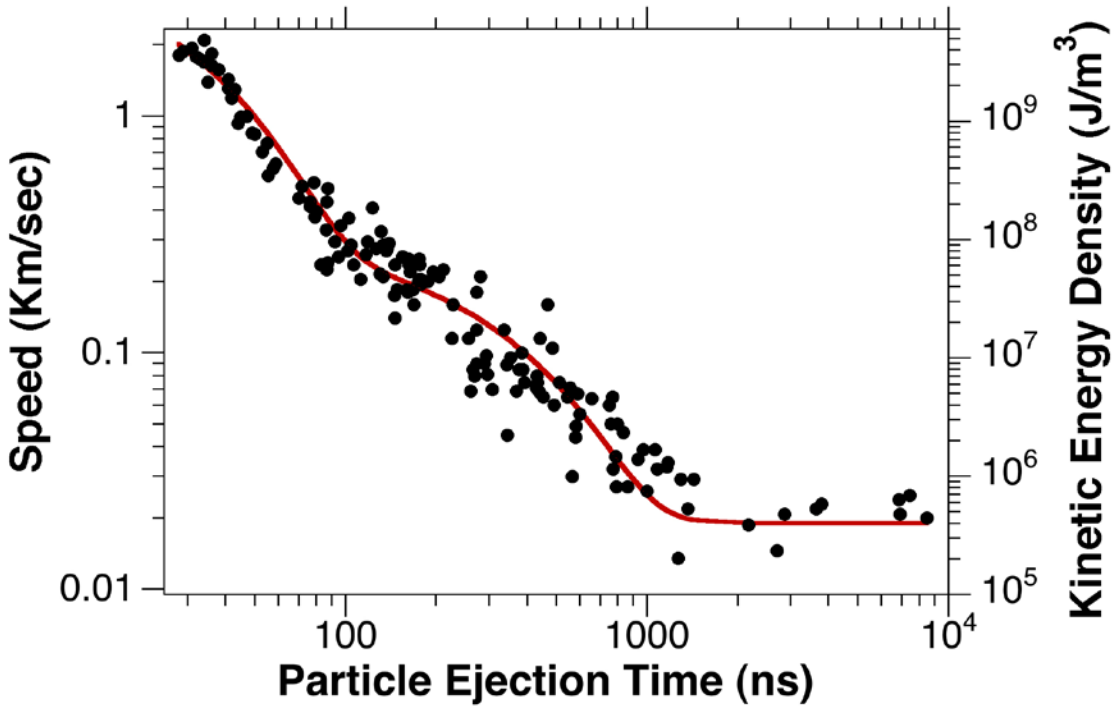

Figure 3: The speed and kinetic energy density of the ejected particles following laser-induced breakdown inside the output surface of fused silica as a function of the estimated ejection time. Line through the experimental data represents an empirical double exponential fit. The kinetic energy density corresponds to the pressure of the superheated material (1 GJ/m^3= 1 GPa) at the time of ejection of the particle.

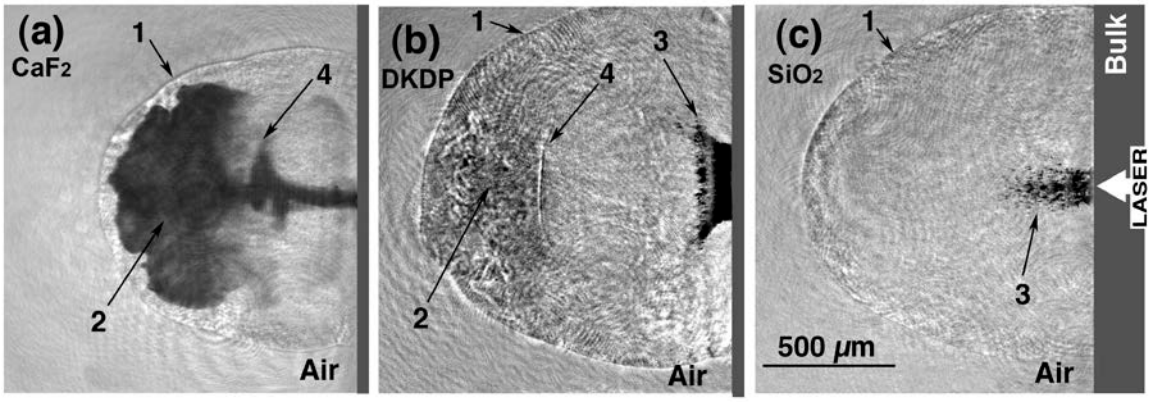

Figure 4: Time resolved images capturing the material ejection at 150 ns delay after exit surface breakdown under 1064 nm, 10 ns at FWHM, ≈250 J/cm^2 average fluence in a) CaF_2, b) $KH_{2-x}D_xPO_4$ and c) SiO_2. Arrows indicate the location of the shockwave (#1), the gaseous material (#2), the microscopic particles (#3) and the delayed secondary pressure wave (#4)

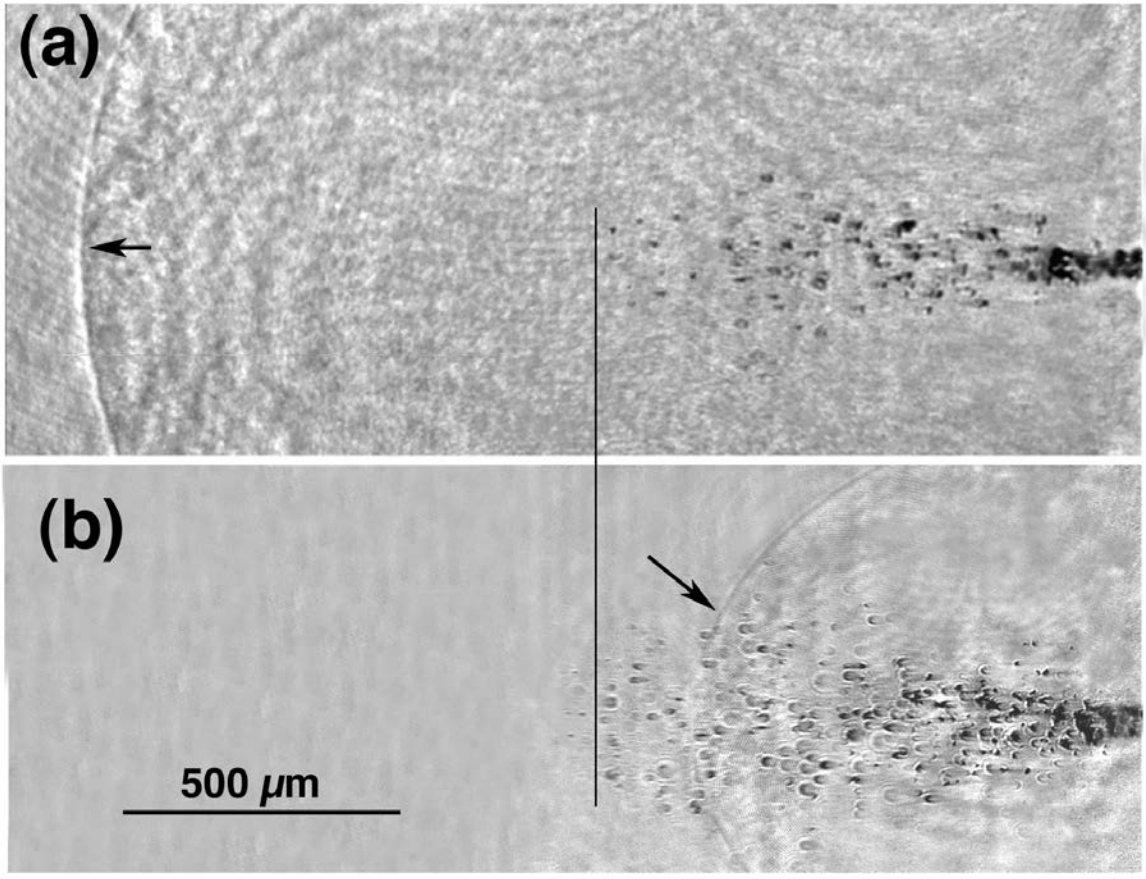

Figure 5. Particle jet captured at 450 nm delay following laser-induced breakdown inside the exit surface of fused silica under laser exposure to a) 1064 nm, 10 ns at FWHM, 300 J/cm^2 average fluence and b) 355 nm, 3 ns at FWHM, 15 J/cm^2 average fluence. Arrows indicate the location of the shock-front and the vertical line the location of the front edge of the jet of ejected particles.